The NASA Optical Communication and Sensor Demonstration Program

Siegfried W. Janson and Richard P. Welle
The Aerospace Corporation
Mail Stop M2/241, P.O. Box 92957, Los Angeles, CA 90009-2957; 310.379.7060
siegfried.w.janson@aero.org

ABSTRACT

The Aerospace Corporation was selected by the NASA Small Spacecraft Technology Program in 2012 to conduct a subsystem flight validation mission to test commercial-of-the-shelf (COTS) components and subsystems that will enable new communications and proximity operations capabilities for CubeSats and other spacecraft. We proposed optical communications using milliradian beam spreads that are compatible with near-term CubeSat pointing capabilities. Our baseline mission will use a ~10-W modulated fiber laser with a 1.4^{o} angular beam-width on a 1.5-U CubeSat (AeroCube-OCSD) and a 30-cm diameter telescope located on Mt. Wilson in southern California to receive optical pulses. We plan on demonstrating the baseline 5-Mbps optical link with a stretch goal of 50-Mbps.

We also proposed integrating an automotive anti-collision radar system and an enhanced optical mouse sensor into these CubeSats to enable future proximity operations. In late 2014 or early 2015, two 1.5-U AeroCube-OCSD CubeSats will be ejected from the same P-POD and brought within 200-meters of each other using on-board GPS for position and velocity determination, variable drag for cooperative orbit rephasing, and cold gas thrusters for proximity maneuvering. Each satellite has deployed wings that allow varying the ballistic coefficient by at least a factor of 4 by changing spacecraft orientation with respect to the flight direction. We plan on characterizing the on-orbit performance of the radar and optical flow sensors as a function of distance between AeroCubes and their orientation.

1.0 NASA'S SMALL SPACECRAFT EFFORTS

The Aerospace Corporation was selected by NASA in 2012 to conduct a subsystem flight validation mission to test commercial-of-the-shelf (COTS) components and subsystems that will enable new communications and proximity operations capabilities for CubeSats and other spacecraft. Our "Integrated Optical Communications and Proximity Sensors for Cubesats" mission, now called the "Optical Communication and Sensor Demonstration" (OCSD), was selected for funding along with the NASA-JPL "Integrated Solar Array and Reflectarray Antenna (ISARA) and Tyvak LLC "CubeSat Proximity Operations Demonstration" (CPOD) flight demonstrations. Our OCSD demonstration will use two 1.5-U CubeSats while ISARA and CPOD use one and two 3-U CubeSats, respectively.

These programs, managed by NASA-Ames Research Center, were originally part of the NASA-Edison program but are now part of NASA's Small Spacecraft Technology Program (SSTP) under the Space Technology Mission Directorate. Other SSTP efforts include PhoneSat and the eight-CubeSat Edison Demonstration of SmallSat Networks (EDSN).[1]

2.0 OPTICAL COMMUNICATIONS FROM LEO

Optical communications exploits the significantly narrower angular antenna beam widths, for a given antenna diameter, for visible through infrared light compared to radio frequency (RF) waves or microwaves. Optical communications systems typically have milli- through microradian angular beam widths while RF/microwave angular widths are measured in tens to thousands of milliradians. Table 1. shows frequencies, wavelength, energy, and minimum angular beam width for a 10-cm diameter antenna at representative UHF, microwave, millimeter, terahertz (sub-mm), visible, and near-infrared frequencies. At UHF, there is no directionality while at near-IR, the theoretical minimum beam spread is only 5.5-microradians. The latter beam spot size at 1000-km range would be only 5.5-meters in diameter. Accurate pointing is essential for long-range optical communications.

Table 1. Representative frequencies, wavelengths, photon energies, and theoretical minimum angular beam widths for radio through visible optical bands using a 10-cm diameter antenna.

Band	Frequency	Wavelength	Energy	Beam Width
UHF	435-MHz	69-cm	1.8-μeV	3.6-rad
S-Band	2.45-GHz	12-cm	10-μeV	0.64-rad
X-Band	10.2-GHz	2.9-cm	42-μeV	0.15-rad
W-Band	77-GHz	3.9-mm	0.3-meV	20-mrad
Sub-mm	0.35-THz	860-μm	1.4-meV	4.5-mrad
Near-IR	283-THz	1.06-μm	1.17-eV	5.5-μrad
Red	460-THz	0.65-μm	1.9-eV	3.4-μrad

The fourth column in Table 1 lists the energy of a representative photon in electron volts. At RF wavelengths, these energies are so small that the quantized nature of light is typically ignored. RF receivers detect incoming signals in the 0.1-to-100 femtowatt range which corresponds to over 10 million photons per bit. Optimized optical receivers, on the other hand, can detect single photons. In practice, typical photoreceivers need between 10 and several hundred photons to identify a bit of information.

2.1 Optical Communications Flight Experiments

Members of The Aerospace Corporation, in collaboration with Tesat-Spacecom, previously demonstrated 5.625-Gbps bidirectional laser communications between a 6.5-cm diameter ground station at the European Space Agency Optical Ground Station in Izana, Tenerife, and a 12.5-cm diameter terminal mounted on the Near Field Infrared Experiment (NFIRE) satellite in low Earth orbit (LEO).[2] The spacecraft terminal had a mass of 35-kg, a power consumption of 120-W, a 0.5 x 0.5 x 0.6-m size, and transmitted 0.7-W at 1064-nm wavelength.[3] This high-performance system with a ~50-microradian angular beam width and gimbaled pointing system would obviously not fit in a CubeSat. Eliminating the optical gimbal and increasing the angular beam width to several milliradians to enable spacecraft body-pointing of the laser would enable a smaller, lighter optical terminal. This takes advantage of the exceptionally low moments-of-inertia of CubeSats, and their ability to perform rapid slew maneuvers.

One example of this simplified laser communications approach is The Very Small Optical TrAnsponder (VSOTA); a downlink-only optical communications system carried on the Japanese RISESat microsatellite. RISESat is much larger than any CubeSat with a mass of 50-kg and a 50 x 50 x 50-cm size. VSOTA transmits at 980 and 1550-nm with output powers of 540 and 80-mW, and angular beam widths of 0.2^o and 0.075^o, respectively.[4] Pointing of the downlink laser at a ground terminal is accomplished by spacecraft rotation, and the required 3-sigma pointing accuracy of RISESAT is 0.1^o. VSOTA is capable of transmitting 10-Mbps to a 20-cm diameter telescope on the ground.

3.0 THE OCSD FLIGHT DEMONSTRATION

Our OCSD effort has two mission requirements:

1. Demonstrate optical communications from a CubeSat to a 30-cm diameter ground station from low Earth orbit (LEO) at a rate of at least 5 Mbps, and
2. Demonstrate tracking of a nearby spacecraft using a commercial, off-the-shelf (COTS) automotive anti-collision radar sensor and an inexpensive optical mouse sensor.

This paper will focus on the first mission requirement, with an additional stretch goal of demonstrating a 50-Mbps optical link to the ground.

3.1 The Spacecraft

The OCSD flight hardware will consist of two, 1.5-U CubeSats that will be ejected from a single CubeSat deployer. We generally improve our attitude control capabilities with each subsequent small satellite build, and plan on sub-degree pointing accuracy for the OCSD spacecraft.

Figure 1 shows a photograph of AeroCube-4C that is currently on-orbit. This 1-U CubeSat has deployable and retractable side wings for variable drag control, a GPS receiver with better than 20-meter spatial accuracy, a 915-MHz transceiver with adaptive data rate up to 0.5-Mbps per second, a distributed computing system, multiple visible cameras with 2-megapixel resolution, an attitude control system with better than 3^o pointing accuracy, and a deployable drag chute. The deployable and retractable wings provide variable drag for orbit control.[5] Figure 2 shows a scheduled photograph of the Moon taken by AeroCube-4C that illustrates our current pointing capability; the Moon (intended target) is about 3^o from the center of the photograph.

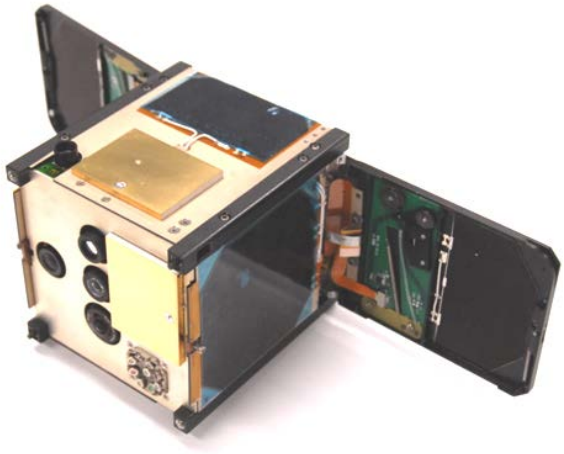

Figure 1. Photograph of the 1-U AeroCube-4C with wings deployed.

Figure 2. AeroCube-4C photograph of the Moon just above Earth's horizon. The Moon should have been in the center of this image.

Attitude sensors on AeroCube-4C include two 2-axis sun sensors with ~0.2° angular error, an Earth nadir sensor with 1° angular error when nadir-pointing, and a 2-axis magnetometer. Magnetometer error was typically about 3° due to magnetic disturbances from the 18650 lithium-ion batteries and reaction wheel assembly. These sensors previously flew on the PicoSatellite Solar Cell Testbed-2 which had a pointing accuracy of about 5°. The improved pointing accuracy on AeroCube-4C is due to enhanced attitude-control software.

AeroCube-5 is an upgraded version of AeroCube-4C with a full three-axis magnetometer and high-accuracy MEMS rate gyros that will launch later this year. AeroCube-6 is currently designed as a spin-stabilized sun-pointing 0.5-U CubeSat that will carry miniaturized radiation dosimeters, an inter-satellite cross-link, an integrated flight computer + GPS receiver + UHF transceiver board, and new attitude sensors into orbit in early 2014. AeroCubes 5 and 6 have their own missions, but will carry components and subsystems as risk-reduction experiments for AeroCube-OCSD.

A schematic rendering of the current AeroCube-OCSD design is given in Figure 3. Instead of deployable and retractable wings for variable drag, this spacecraft has deployed and locked wings. Attitude control, relative to the flight direction, provides at least a 4:1 ratio in drag. This feature, plus an on-board cold gas thruster with a ~10-m/s ΔV capability, enables proximity operations between the two individual spacecraft.

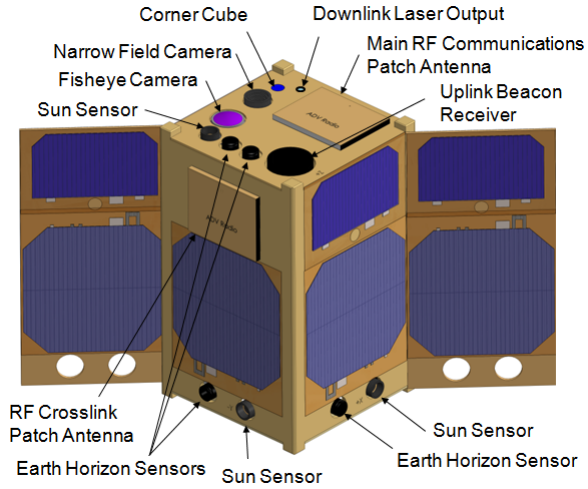

Figure 3. Schematic rendering of AeroCube-OCSD.

Optical communications requires attitude control with better than 1° pointing accuracy. The AeroCube-OCSD spacecraft have multiple sun and Earth horizon sensors that allow continuous Earth nadir sensing and continuous sun direction sensing when not eclipsed by the Earth. The Earth horizon sensors are based on commercially-available Melexis MLX-90620 4 x 16 array optical thermometers while the sun sensors are based on our flight-proven quad photodiode design with an increased field-of-view.[6] The Earth horizon sensors should have an accuracy of 0.5° while the sun sensor accuracy should remain at 0.2° based on laboratory testing.

The two-chip magnetometer in AeroCube-4C that had sensor orthogonality and bond pad soldering issues has been replaced by a single chip HMC5883L magnetometer from Honeywell.[7] This magnetometer will be flight-tested on AeroCube-6. In addition, we discovered that the 18650 lithium-ion batteries used on AeroCube-4C had a significant (0.02-A-m^2) magnetic

dipole moment. This residual field, plus the concentration of the Earth's magnetic field along the cylindrical battery shell, resulted in the rather large ~3° magnetic orientation errors. For AeroCube-OCSD, we will degauss the batteries and locate them as far as possible from the magnetometers to reduce magnetic sensing errors to 1° or less. A backup magnetometer will be mounted to one deployed wing to further remove magnetic field sensing from the spacecraft bus.

To augment 3-axis attitude information during eclipse, we will use a Sensonor STIM-210 3-axis rate gyro.[8] This device can provide 0.6° of inertial error during 40-minutes of eclipse if a 15-minute bias calibration is performed during the previous sunlit portion of the orbit. These devices can be susceptible to helium exposure that can occur during launch vehicle preparations, so we will mount them inside their own hermetically-sealed container.

AeroCube-4C has multiple 1/3" 2-megapixel imagers that are typically used to verify spacecraft orientation relative to Earth. We tested their potential use as star trackers by taking images free of solar and Earth light interference and processing them on the ground using an algorithm developed by The Aerospace Corporation. One camera with a 16-mm focal length, F/2.0 lens was able to see stars below 5th magnitude after image processing. This image processing step is being ported to a field-programmable gate array to provide stellar positions to a microprocessor for attitude determination at 1-Hz. Unlike "lost in space" algorithms, we will take advantage of magnetometer and other sensor attitude data to significantly reduce the search space. We expect to obtain 0.02° attitude knowledge using our existing optics, camera chips, and algorithms.

The final attitude sensor for AeroCube-OCSD is an uplink beacon receiver to provide closed-loop pointing control at the optical ground station. This sensor consists of a quad photodiode at the focal plane of a 2.5-cm diameter lens. A 10-nm bandpass filter in front of the lens filters out 99% of sunlight, Earthlight, and Moonlight. Photocurrents from each diode quadrant are measured, and differences in current between the four segments provides incoming angle information along 2-axes. The combined signal from all quadrants is used to receive optical uplink data. This sensor can have an angular accuracy of 0.1°.

Table 2 shows four different attitude control modes for optical communications, their estimated pointing accuracy, and impact on data rates. Having these four sensor modes enables a basic 5-Mbps optical downlink with failure of any single attitude sensor system.

Table 2. Attitude control modes for optical communications, expected pointing accuracy, and use.

Mode	Sensors	Pointing Accuracy	Use
Sunlit open loop	Sun and Earth horizon	~0.6°	5-Mbps link when sunlit
Eclipsed open loop	Earth horizon, magnetometers, and rate gyros	~0.7°	5-Mbps link when eclipsed
Star tracker open loop	Magnetometers and star trackers	~0.1°	50-Mbps link without uplink beacon
Closed loop	Uplink receiver and magnetometers	~0.2°	50-Mbps link with uplink beacon

Attitude actuators include a triad of magnetic torque rods and a triad of reaction wheels. Our torque rods, to be flight tested on AeroCube-6, have a magnetic moment of 0.2-A-m^2. They provide torques for detumbling and reaction wheel unloading. The reaction wheels, shown in Figure 4, have flight heritage on our AeroCube-4 series spacecraft. They provide primary attitude control within 0.1° with 1-mN-m-s of total angular momentum storage and fit within a 2.5-cm cubic volume. Spacecraft slew rates can be in excess of 5° per second. Note that the pointing accuracy values in Table 2 include the 0.1° attitude actuation accuracy.

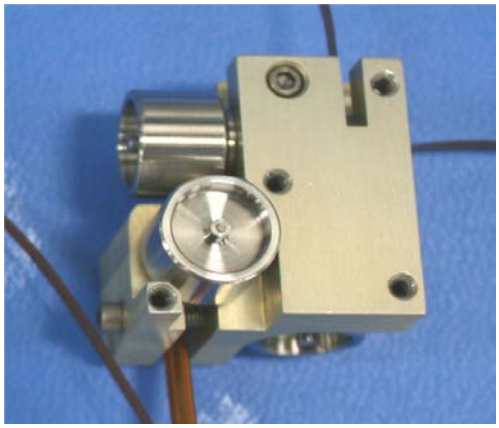

Figure 4. Photograph of our 3-axis reaction wheel assembly.

3.2 The Optical Downlink Generator

Our optical downlink will use a low-power amplitude-modulated diode laser followed by two polarization-maintaining ytterbium-doped fiber amplifier stages. A breadboard test demonstrated 14.7-W of average output power at 1064-nm using 55-W input power. The 5-ns

pulses were at a 1-MHz rate, and this system is capable of generating pulse rates greater than 100-MHz at the same efficiency (25% optical output/input). We subsequently fabricated a brassboard version with a 1 x 9 x 9-cm volume that readily fits into our payload volume. The laser downlink generator will be powered by a dedicated lithium-ion battery capable of providing 60-W power levels over a maximum 180-s period for at least 100 charge/discharge cycles.

3.3 The Optical Ground Station

We will use our Mobile Communications and Atmospheric Measurements (MOCAM) station located at Mt. Wilson, CA, as our primary optical ground station. This facility is within 50-km of our El Segundo campus and was used for tracking NFIRE. Figure 5 shows a photograph of a Meade 30-cm-diameter telescope mounted on a high-precision gimbal system that allows tracking of LEO spacecraft.

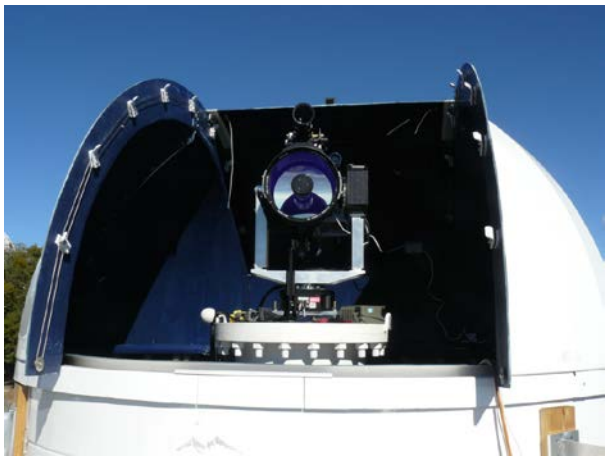

Figure 5. Photograph of our 30-cm diameter Meade receive telescope in our MOCAM optical ground station.

The optical ground station receive telescope will have an avalanche photodiode detector at its focus, and an avalanche quad photocell to provide off-angle error signals for closed-loop satellite tracking. Rough satellite tracking will use high-accuracy ephemerides generated from spacecraft GPS fixes on previous orbits. Our ground station network currently consists of three internet-connected RF ground stations located in El Segundo, California, College Station, Texas, and Gainsville, Florida.

The top three tracking modes in Table 2 rely on spacecraft attitude and inertial sensors to provide open-loop attitude knowledge for pointing the downlink beam at the ground station. The last mode relies on open-loop attitude knowledge to roughly point at the ground station, and then use a position-sensitive (the quad photodiode) beacon detector to lock onto the uplink to provide closed-loop pointing. Pointing accuracy, based on our experience with quad cell sun sensors and our reaction wheels is estimated at ~0.2^o. The uplink beacon will be a ~10-W laser from a separate 20-cm diameter telescope that is mounted to the primary Meade. Although this complicates the ground station and adds local eye-safety issues, it provides a signal for robust closed-loop pointing control to the AeroCube.

3.4 The Optical Link Budget

Our 10-W class laser downlink enables useful data rates within the typically crude pointing accuracy of CubeSats. The baseline 5-Mbps demonstration is an order-of-magnitude faster than our current AeroCube communications capabilities, and the 50-Mbps stretch goal will enable new mission capabilities for CubeSats. Table 3 shows optical downlink budgets for the 5- and 50-Mbps links using a 30-cm diameter ground telescope, an APD photoreceiver with an expected sensitivity of 200 photons/bit, and a range of 900-km. For these parameters, we get a ~3-X (5-dB) positive link margin for both cases. Note that table 3 shows calculated link budgets for reception at the half-power radius on the ground; this corresponds to off-pointing by 0.7^o and 0.25^o, respectively, for the 5-Mbps and 50-Mbps links. Higher data rates can be achieved with better pointing, by increasing the ground telescope aperture, or by increasing photoreceiver sensitivity.

Table 3. Optical downlink link budgets

Parameter	5-Mbps	50-Mbps
FWHM angle (degrees)	1.4	0.5
Wavelength (nm)	1064	1064
Output Power (W)	14	14
Atmospheric Transmission	0.8	0.8
Telescope Collection Efficiency	0.5	0.5
Half-Max Radius at Range (km)	11.2	3.9
Half-Max Irradiance at Range (W/m^2)	2.0 x 10^{-8}	1.6 x 10^{-7}
Half-Max Photons per Bit:	740	610

Table 3 shows that our baseline 5-Mbps link requires a downlink pointing accuracy of 0.7^o, while the 50-Mbps link requires a pointing accuracy of 0.25^o. The baseline

link can be accomplished using any of the modes in Table 1 while the 50-Mbps stretch goal can only be accomplished using the star tracker or uplink beacon. We are currently evaluating how to provide 0.5° and 1.4° FWHM beams on each spacecraft with minimum risk.

3.5 Optical Communications Concept of Operations

The first step in the flight demonstration is to identify an AeroCube pass with at least 180-seconds of less than 900-km range between MOCAM and the satellite. For a nominal 500-km altitude circular orbit, this corresponds to elevation angles higher than 30°. This pass should occur at least twelve hours in the future to enable generation of time-stamped spacecraft pointing tables for the optical pass, and to fully charge spacecraft batteries. The next step is to verify clear weather conditions for this pass, and to check that the sun-to-spacecraft angular separation is sufficient to prevent downlink detector saturation.

Once the pass is identified, AeroCube-OCSD-A or -B will be commanded to obtain multiple (9) GPS fixes over an orbit and to download that data on the next available pass over one of our RF ground stations. Ground-based processing of these GPS fixes will generate high-precision orbit ephemerides that will be used by the optical ground station to track the satellite, and by ground-based computers to generate a time-stamped pointing table for the AeroCube. Our GPS receiver has a ~20-meter position accuracy, and by processing nine positions per orbit over two days, we've generated high-precision ephemerides with initial errors of 7, 3.5, and 2-meters in the in-track, cross-track, and radial directions, respectively (see ref. 5). The pointing table will be uploaded to the appropriate AeroCube at least one orbit before the appointed pass.

During this last orbit, the spacecraft will set its on-board clock using GPS time and calibrate its on-board rate gyros to minimize bias drift errors. As it rises above the horizon, the spacecraft will be pointing at the ground station using one of the open-loop modes listed in Table 2. The optical ground station will track the rising satellite in open loop mode and activate the optical uplink beacon if required. Once calibrated against stellar targets, our optical ground station tracking errors are expected to be less than 10-meters at the satellite when using recent high-precision orbital ephemerides. This tracking error maps to a 33-micron position error at the focal plane of a 3-meter focal length telescope at 900-km range. The APD detector at the focal plane of the telescope should therefore have a diameter of at least 80-microns.

When the satellite reaches an elevation of at least 20°, it will turn on the downlink laser and transmit a continuous pulse train. Our rather broad milliradian-class angular beamwidths enable open-loop pointing at the ground station; our 1.4° FWHM downlink beam for a 5-Mbps data rate produces an 11-km diameter spot at 900-km range. The spacecraft can also perform pre-programmed angular scans to find the ground station when using narrower, higher data-rate, downlink beams in open loop mode. Once the spacecraft and ground station are aimed at each other, link testing and establishment of bit error rates under various conditions will occur until the range exceeds 900-km.

4.0 OTHER PAYLOADS

4.1 Proximity Operations

While the optical communications demonstrations can be performed independently on each spacecraft, the remaining payload demonstrations require proximity operations between two spacecraft. Design and implementation of the rephasing and proximity operations are beyond the scope of this paper, but the general concept follows:

In late 2014 or early 2015, two 1.5-U AeroCube-OCSD CubeSats will be ejected from the same P-POD and brought within 200-meters of each other using on-board GPS for relative position and velocity determination, variable drag for cooperative orbit rephasing, and cold gas thrusters for proximity maneuvering. Each satellite has deployed wings that allow varying the ballistic coefficient by at least a factor of 4 by changing spacecraft orientation with respect to the flight direction as shown in Figure 6. Variable-drag rephasing is expected to occur over a period of one to three weeks, depending on initial ejection altitude.

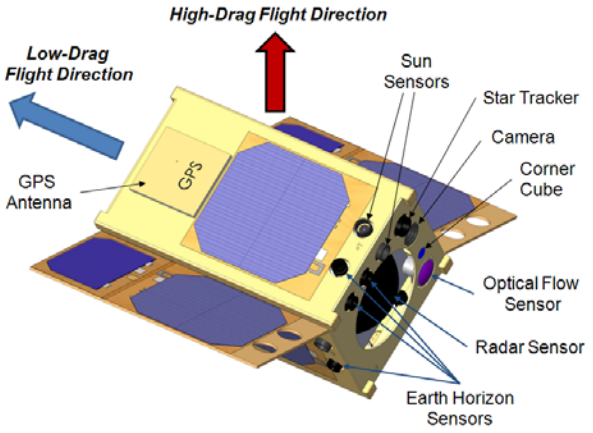

Figure 6. High-drag and low-drag orientations for AeroCube-OCSD.

4.2 Radar and Optical Flow Sensors

Figure 6 also shows placement of the radar and optical flow sensors, the star tracker, and an additional camera to monitor proximity operations. The radar is an automotive adaptive-cruise-control sensor with a terrestrial range of about 200-meters. These 77-GHz radars generate a 5^o x 30^o fan-shaped beam to provide range, range rate, and azimuth angle (angle from bore sight in the wide beam direction) for multiple targets within their field-of-view. We will test their utility for general proximity and potential docking operations by bringing the two AeroCube-OCSD spacecraft together within 200-meters, aiming the radars at each other, and tracking each other while taking images and logging GPS positions for each spacecraft. We plan on characterizing the on-orbit performance of the radar and optical flow sensor as a function of distance between AeroCubes and their orientation.

The optical flow sensor is an optical mouse sensor with an 18 x 18-pixel image sensor coupled with a digital signal processor (DSP) on the same die. Figure 7 shows a photograph of the silicon die in an Avago ADNS-2620 optical mouse sensor.[9] The ~1-mm-square detector array is on the left, and the signal processing electronics are on the right. In the mouse application, a laser or LED illuminates the mouse pad below it and a portion of the surface is imaged directly on the pixel array. The DSP monitors how image features move over time and outputs pad velocity, with respect to the sensor, as V_x and V_y speeds. If the myopic mouse lens is replaced with a larger lens that is focused at infinity, this sensor will indicate X- and Y- angular rates for the imaged scene. This is the basis for our patent-pending flight-direction sensor flown on AeroCube-4.[10] The sensor is aimed at nadir using horizon sensors, and the Earth becomes our mouse pad.

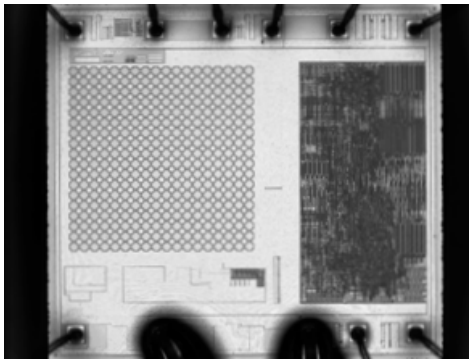

Figure 7. Photograph of the Avago ADNS-2620 silicon die.

For OCSD we will use this sensor to provide angular tracking rates, with respect to the host spacecraft body, of the neighboring AeroCube when it is lit by sunlight. The lens should be at least 2.5-cm in diameter to provide enough light to the mouse sensor chip.

5.0 SUMMARY

The NASA OCSD effort is a subsystem flight validation mission to test commercial-of-the-shelf components and subsystems that will enable new communications and proximity operations capabilities for CubeSats and other spacecraft. It will demonstrate optical communications using milliradian beam spreads that are compatible with near-term CubeSat pointing capabilities. The baseline mission will use a ~10-W modulated fiber laser with a 1.4^o angular beam-width on a 1.5-U CubeSat (AeroCube-OCSD) and a 30-cm diameter telescope located on Mt. Wilson in southern California to receive optical pulses. We plan on demonstrating the baseline 5-Mbps optical link with a stretch goal of 50-Mbps. In addition, the spacecraft will also flight test an anti-collision radar system and an enhanced optical mouse sensor to enable future proximity operations.

In late 2014 or early 2015, two 1.5-U AeroCube-OCSD CubeSats will be ejected from the same P-POD and brought within 200-meters of each other using on-board GPS for position and velocity determination, variable drag for cooperative orbit rephasing, and cold gas thrusters for proximity maneuvering. Each satellite has deployed wings that can change the ballistic coefficient, for variable drag control, by at least a factor of 4. We plan on characterizing the on-orbit performance of the radar and optical flow sensors as a function of distance between AeroCubes, their configuration (wings open and closed), and their orientation.

References

1. H. Smith, S. Hu, and J. Cockrell, "NASA's EDSN Aims to Overcome the Operational Challenges of CubeSat Constellations and Demonstrate an Economical Swarm of 8 CubeSats Useful for Space Science Investigations," paper SSC-XI-2, AIAA/USU Small Satellite Conference, Logan, Utah, August 10-15, 2013.

2. Fields, R., Kozlowski, D., Yura, H., Wong, R., Wicker, J., Lunde, C., Gregory, M., Wandernoth, B., and Heine, F., "5.625 Gbps Bidirectional Laser Communications Measurements Between the NFIRE Satellite and an Optical Ground Station," Proc. of the 2011 Int. Conf. on Space Optical Systems and Applications, pp.44-53, Santa Monica, CA, 11-13 May, 2011.

3. Heine, F., Kampfner, H., Lange, R., Czichy, R., Meyer, R., and Lutzer, M., “Optical Inter-Satellite Communication Operational,” 2010 Military Communications Conference, pp.1583-1587, San Jose, CA, Oct. 31 – Nov. 3, 2010.

4. Kubo-oka, T., Kunimori, H., Takenaka, H., Fuse, T., and Toyoshima, M., “Optical Communication Experiment Using Very Small Optical TrAnsponder Component on a Small Satellite RISESAT,” Proc. Of the Int. Conf. on Space Optical Systems and Applications (ICSOS), 2012, Ajaccio, Corsica, France, Oct. 9-12, 2012.

5. J. Gangestad, B. Hardy, and D. Hinkley, “Operations, Orbit Determination, and Formation Control of the AeroCube-4 CubeSats,” paper SSC13-X-4, AIAA/USU Small Satellite Conference, Logan, Utah, August 10-15, 2013.

6. Melexis Microelectronic Systems, MLX90620 datasheet, URL: http://www.melexis.com/Assets/Datasheet-IR-thermometer-16X4-sensor-array-MLX90620-6099.aspx, Melexis Microelectronic Systems, Ieper, Belgium, May 2013.

7. Honeywell, 3-Axis Digital Compass IC datasheet, URL: http://www51.honeywell.com/aero/common/documents/myaerospacecatalog-documents/Defense_Brochures-documents/HMC5883L_3-Axis_Digital_Compass_IC.pdf, Honeywell, Plymouth, MN, May 2013.

8. Sensonor AS, Butterfly Gyro STIM210 Multi-Axis Gyro Module datasheet, URL: http://www.sensonor.com/media/90317/datasheet%20stim210%20ts1545.r10.pdf, Sensonor AS, Horton, Norway, May 2013.

9. Avago Technologies, ADNS-2620 Optical Mouse Sensor Product Overview, Avago Technologies Limited, San Jose, CA, URL: http://www.avagotech.com/docs/AV02-1119EN May 2013.

10. Janson, S., and Fuller, J, “Systems, Methods, and Apparatus for Sensing Flight Direction of a Spacecraft,” U.S. patent application 20120109425, May 3, 2012.